MOLECULAR AND CELLULAR BIOLOGY, Feb. 2005, p. 1191–1199 Vol. 25, No. 3
0270-7306/05/$08.00+0 doi:10.1128/MCB.25.3.1191–1199.2005

TIEG1 Null Mouse-Derived Osteoblasts Are Defective in Mineralization and in Support of Osteoclast Differentiation In Vitro

Malayannan Subramaniam,[1]* Genevieve Gorny,[1] Steven A. Johnsen,[2] David G. Monroe,[1] Glenda L. Evans,[3] Daniel G. Fraser,[4] David J. Rickard,[5] Kay Rasmussen,[1] Jan M. A. van Deursen,[6] Russell T. Turner,[3] Merry Jo Oursler,[4] and Thomas C. Spelsberg[1]

Department of Biochemistry and Molecular Biology,[1] Orthopedic Research,[3] Department of Pediatric and Adolescent Medicine,[6] and Division of Endocrinology, Department of Internal Medicine,[4] Mayo Clinic College of Medicine, Rochester, Minnesota; Zentrum für Molekulare Neurobiologie, Universität Hamburg, Hamburg, Germany[2]; and Musculoskeletal Diseases Biology, GlaxoSmithKline, Collegeville, Pennsylvania[5]

Received 25 May 2004/Returned for modification 4 August 2004/Accepted 4 November 2004

Transforming growth factor β-inducible early gene 1 (TIEG1) is a member of the Krüppel-like transcription factor family. To understand the physiological role of TIEG1, we generated TIEG$^{-/-}$ (null) mice and found that the TIEG$^{-/-}$ mice had increased osteoblast numbers with no increased bone formation parameters. However, when calvarial osteoblasts (OBs) were isolated from neonatal TIEG$^{-/-}$ and TIEG$^{+/+}$ mice and cultured in vitro, the TIEG$^{-/-}$ cells displayed reduced expression of important OB differentiation markers. When the OBs were differentiated in vitro by treatment with bone morphogenic protein 2, the OBs from TIEG$^{+/+}$ calvaria displayed several mineralized nodules in culture, whereas those from TIEG$^{-/-}$ mice showed no nodules. To characterize the OBs' ability to support osteoclast differentiation, the OBs from TIEG$^{+/+}$ and TIEG$^{-/-}$ mice were cultured with marrow and spleen cells from TIEG$^{+/+}$ mice. Significantly fewer osteoclasts developed when TIEG$^{-/-}$ OBs were used to support osteoclast differentiation than when TIEG$^{+/+}$ OBs were used. Examination of gene expression in the TIEG$^{-/-}$ OBs revealed decreased RANKL and increased OPG expression compared to TIEG$^{+/+}$ OBs. The addition of RANKL to these cocultures only partially restored the ability of TIEG$^{-/-}$ OBs to support osteoclast differentiation, whereas M-CSF alone or combined with RANKL had no additional effect on osteoclast differentiation. We conclude from these data that TIEG1 expression in OBs is critical for both osteoblast-mediated mineralization and osteoblast support of osteoclast differentiation.

Krüppel-like transcription factors (KLFs) are DNA-binding transcriptional regulators which contain C_2, H_2-type zinc fingers and play important roles in regulating biological processes such as cell growth, differentiation, and embryogenesis (1, 5, 32). The number of members of the KLF family has been increasing, and it is estimated that 1% of the human genome might contain this family of regulatory factors (5, 11). Our laboratory has cloned a member of this family, the transforming growth factor β (TGF-β)-inducible early gene 1 (TIEG1), since it represented a primary response gene to TGF-β treatment in human osteoblasts (28). Cook et al. (4) identified TIEG2, which shares 91% homology with TIEG1 within the zinc finger region but only 44% homology at the N terminus region. They also showed evidence that overexpression of TIEG2 in Chinese hamster ovary cells inhibits cell proliferation. Recently, Wang et al. (36) identified another member of the TIEG family, TIEG3, which has properties similar to those of TIEG1 and TIEG2.

A better understanding of the mechanism of action of TIEG1 is evolving. Using a GAL4-based transcriptional assay, Cook et al. (4) demonstrated that TIEG1 protein has three repression domains. Studies by Zhang et al. (39) identified an alpha-helical repression motif located within the repression domain of TIEG1 and TIEG2. These authors have also shown evidence that these motifs mediate the direct interaction of TIEG1 with mSin3A, which mediates the repression of target genes. Our laboratory has shown that TIEG1 overexpression enhances the TGF-β induction of Smad-binding element reporter activity via TIEG1 repression of the inhibitory Smad7 gene activity (14). Studies from our laboratory also identified an E_3 ubiquitin ligase, seven in absentia homologue 1 (SIAH1), as a major TIEG1 interacting protein (15). Targeting TIEG1 for proteosomal degradation by SIAH1 explains the rapid turnover of the TIEG1 protein and may serve to limit the duration and magnitude of TGF-β response in target cells. Recently, Noti et al. (20) demonstrated that the TIEG can act as an inducer of gene transcription via upregulating the CD11d gene expression after differentiation of myeloid cells with an increased binding of TIEG1 to CD11d promoter, suggesting CD11d gene as a target for TIEG1.

Estrogen, an important anabolic hormone in bone, has also been shown to induce TIEG1 mRNA in human osteoblasts (31). Also, several of the TGF-β superfamily members induce TIEG1 mRNA and protein levels within 2 h of the growth factor treatment in human osteoblasts and other cell types (28). TIEG1 overexpression in MG63 human osteosarcoma

* Corresponding author. Mailing address: Department of Biochemistry and Molecular Biology, 1601B Guggenheim Bldg., Mayo Clinic College of Medicine, 200 First St., S.W., Rochester, MN 55905. Phone: (507) 284-4909. Fax: (507) 284-2053. E-mail: subramaniam.malayannan@mayo.edu.

cells mimics TGF-β effects by increasing alkaline phosphatase and decreasing osteocalcin secretion (10). Previously, we demonstrated that TIEG1 mRNA and protein are expressed in many human tissues; however, expression was limited to specific cell types within those tissues (29). In the same study, TIEG1 protein levels were shown to be markedly reduced in metastatic human breast cancer tissues compared to normal breast epithelia, with the levels correlating with the stage of the disease. A recent study by Reinholz et al. (22) that used quantitative reverse transcription-PCR (RT-PCR) supported these studies, demonstrating that TIEG1 mRNA levels are significantly reduced in breast cancer tissue. The mRNA levels accurately discriminated between normal breast tissue and primary tumors with a maximum sensitivity and specificity of 96 and 93%, respectively. TIEG1 has been implicated in the signaling process that mediates apoptosis in HL-60 cells by homoharringtonine (13). In addition, TIEG1 overexpression in pancreatic carcinoma, hepatocarcinoma, and mink lung epithelial cells inhibited cell growth and induced apoptosis similar to that of TGF-β treatment (3, 23, 30). These data suggest that TIEG1 might be a tumor suppressor.

To elucidate the function of TIEG, we report here the development of a TIEG1 knockout mouse line by targeting disruption of the TIEG1 gene. In vivo analysis of bone parameters revealed that TIEG$^{-/-}$ mice had increased osteoblasts per bone surface without an increase in any bone formation and, further, the osteoblasts isolated from TIEG1$^{-/-}$ mice are defective in two important osteoblast functions, mineralization and support of osteoclast differentiation, compared to wild-type mice. Our data indicate that these defects are most likely due to altered gene expression in the TIEG$^{-/-}$ OBs.

MATERIALS AND METHODS

Construction of TIEG1 targeting vector. TIEG1$^{-/-}$ embryonic stem (ES) cells were developed in collaboration with Incyte Genomics (St. Louis, Mo.). The murine TIEG1 gene was cloned from a mouse 129/Sv ES cell library in P1 phage by using a PCR-based screen with primers designed to target a conserved region of the mouse and human TIEG1 cDNAs. The resulting clone was digested with EcoRI to yield a 14-kb fragment containing the full-length coding region. The entire fragment was mapped and sequenced and found to contain four exons and three introns covering 7.1 kb, bounded by 6.6 kb of 5′-flanking and 0.9 kb of 3′-flanking sequence. The targeting vector was constructed by ligating a 3.5-kb XbaI fragment of the 5′-flanking region (the 5′ arm) upstream of the neomycin resistance cassette in vector 38loxPNeo and a 3.3-kb MscI-XbaI region containing exons 3 and 4 (the 3′ arm) downstream from Neo (Fig. 1A). The complete targeting construct of 10.3 kb was then excised from the resulting vector, 38loxPNeo/TIEG.

Bone histomorphometry. Tibiae were dehydrated by daily changes of ethanol (1 day in 95% and 6 days in 100%) before infiltration with a methylmethacrylate mixture (methylmethacrylate-2-hydroxyethyl and methylmethacrylate [12.5:1]). Undecalcified bones were embedded in the methylmethacrylate, and longitudinal sections (5 μm) were cut from the center of the proximal tibiae with a microtome (model 2065; Reichert Jung, Heidelberg, Germany) as previously described (33, 34).

All tissue measurements were performed with the OsteoMeasure Analysis System (OsteoMetrics, Atlanta, Ga.), which consists of a Pentium 133 computer coupled to a photomicroscope and image analysis system. This image system includes a high-resolution color video camera (Sony DXC-970 MD) that transmits the image of the specimen through a microscope (BH-2; Olympus, New Hyde Park, N.Y.) to a video monitor that registers the movement of a digitizing mouse on a graphics tablet (OsteoTablet; OsteoMetrics). The regions of interest, e.g., bone perimeters, cell numbers, and fluorochrome labels, are traced by the operator; lengths of tracings, areas enclosed by traced lines, and average distances between traced lines are calculated automatically by the software. All histomorphometry data are generated and derived in accordance with standardized formulae, methods, and nomenclature (21).

OB isolation. Calvarial osteoblasts (OBs) were isolated from 1- to 3-day-old neonatal mouse pups. In brief, 1- to 3-day-old mouse pups that were born to heterozygous TIEG1 null C57BL/6/129 parents were euthanized by using CO_2. The calvarium was removed and washed several times with phosphate-buffered saline (PBS) to remove the blood cells. The calvaria were minced and digested in Hanks balanced saline solution containing bovine serum albumin (4 mg/ml) and collagenase type 2 (4 mg/ml) for 10 min at 37°C. The cells obtained from the third digest was centrifuged at 221 × *g* for 5 min, and the cells were resuspended in α-minimal essential medium containing 10% fetal bovine serum and grown in culture dishes. The OBs thus obtained were used as support cells for osteoclast precursors and for osteoblast differentiation studies.

Osteoblast mineralization studies. Primary OBs obtained from TIEG$^{+/+}$ and TIEG$^{-/-}$ mice were plated onto 12-well plates at a low density and grown until confluency. The cells were then shifted to differentiation media containing ascorbic acid (50 μg/ml) and β-glycerol phosphate (4 mM). The cells were treated with vehicle or bone morphogenic protein 2 (BMP2; 100 ng/ml) every third day and allowed to mineralize for 18 days. Once the bone nodules were visible, the cells were washed twice with PBS and fixed in 10% neutral buffered formalin overnight. The fixed cells were stained with 2% (wt/vol) alizarin red for 10 min. Finally, the cells were washed with distilled water to remove excess stain and visualized for bone nodules.

Northern blot analysis and semiquantitative RT-PCR. Northern blot analysis to measure the TIEG1 mRNA levels in TIEG$^{+/+}$ and TIEG$^{-/-}$ osteoblasts were performed as described previously (28). Semiquantitative RT-PCR was performed to measure the osteoblast-specific marker genes in cultured OBs, as described previously (24). The primers used were as follows: mTIEG-F, 5′-GTCTCAGTGCTCCCGTCTGT-3′; mTIEG-R, 5′-CCACCGCTTCAAAGTCACTC-3′; alkaline phosphatase-F, 5′-TCTCAACTGTTCTAGTTCCT-3′; alkaline phosphatase-R, 5′-TTGGGTCATTTCCACATGC-3′; type 1A Col.-F, 5′-TCTCCACTCTTCTAGTTCCT-3′; type 1A Col.-R, 5′-TTGGGTCATTTCCACATGC-3′; ostrix-F, 5′-TGAGGAAGAAGCCCATTCAC-3′; ostrix-R, 5′-ACTTCTTCTCCCGGGTGTG-3′; osteocalcin-F, 5′-TCTGACAAACCTTCATGTCC-3′; osteocalcin-R, 5′-AAATAGTGATACCGTAGATGCG-3′; GAPDH-F, 5′-CACCATGGAGAAGGCCGGGG-3′; and GAPDH-R, 5′-GACGGACACATTGGGGGTAG-3′.

^{35}S labeling and immunoprecipitation. TIEG$^{+/+}$ and TIEG$^{-/-}$ OBs were grown in culture. When the cells were 90% confluent, the cells were washed and placed in serum-free medium for 24 h. After serum starvation, the cells were placed in methionine-free labeling medium. [^{35}S]methionine (150 μCi/ml) was added to the medium, along with TGF-β_1 (2 ng/ml), and the cells were labeled for 3 h. After labeling, the cells were lysed in radioimmunoprecipitation assay buffer (10 mM sodium phosphate, 150 mM sodium chloride [pH 7.4], 1% [wt/vol] NP-40, 0.5% [wt/vol] sodium deoxycholate, 0.1% [wt/vol] sodium dodecyl sulfate) containing protease inhibitor cocktail mix (Roche Diagnostics, Mannheim, Germany). The cell lysates were immunoprecipitated with 8 μg of TIEG1-specific polyclonal antibody. The immunoprecipitates were separated by sodium dodecyl sulfate-polyacrylamide 10% ([wt/vol]) gel electrophoresis, and the gel was soaked in Autofluor (National Diagnostics, Atlanta, Ga.), dried, and exposed to an X-ray film.

Cell proliferation assay. TIEG$^{+/+}$ and TIEG$^{-/-}$ OBs were seeded at 6,400 cells/well on 96-well plates and grown for 24, 48, and 72 h at 37°C. The proliferation of these cells was measured by using the Cell Titer 96 Aqueous One solution cell proliferation assay (Promega, Madison, Wis.). Average results from six replicates were compared between TIEG$^{+/+}$ and TIEG$^{-/-}$ OBs.

Southern blot analysis and genotyping. Genomic DNA was isolated from mouse tail by using a DNeasy tissue kit (QIAGEN, Valencia, Calif.). Twenty micrograms of the genomic DNA was digested with EcoRI and separated on a 0.8% (wt/vol) agarose gel. Southern blot analysis was performed with digested DNA as described by Sambrook et al. (26). The blot was probed with ^{32}P-labeled 5′ probe, an 0.8-kb EcoRI/XbaI fragment from subclone Eco-TIEG.

Genotyping by PCR was performed with the following primers: KONEOF1, 5′-CTA AAG CGC ATG CTC CAG ACT GCC-3′; intron 2F, 5′-CCT CTA ATT CCT CTC CTT GC-3′; and exon 3R1, 5′-TGG TGG TTG CAC AGT TGG GCA TCA GCT G-3′.

PCR was performed for 1 min at 94°C, 2 min at 55°C, and 3 min at 72°C for a total of 40 cycles. The PCR products were separated on a 1.5% agarose gel, and the gels were stained with ethidium bromide and photographed.

In vitro osteoclast differentiation with calvarial support cells. Calvarial cells were plated at 4 × 10^4 cells/well on a 48-well plate (Fisher, Pittsburgh, Pa.) 24 h prior (day 1) to the addition of osteoclast precursors (1.5 × 10^6 marrow mononuclear cells or 4.8 × 10^7 spleen cells per plate) harvested as we have described

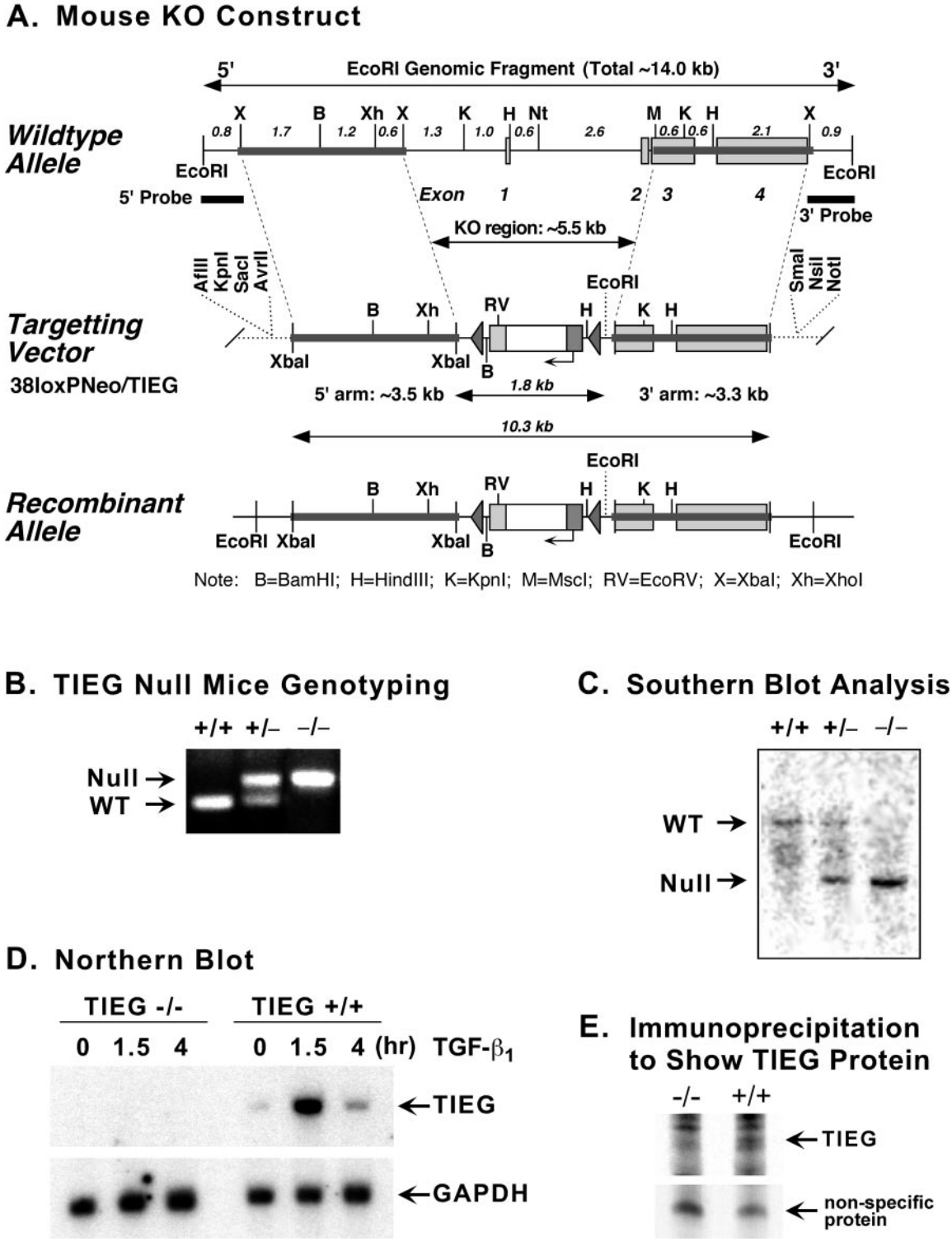

FIG. 1. Mouse knockout construct and verification of TIEG1 null mutation. (A) Generation of the TIEG1 null allele (bottom panel) by homologous recombination between the targeting vector (middle panel) and wild-type allele (top panel). In the recombinant allele, the 1.8-kb Neo^r cassette replaces ca. 5.5 kb of genomic TIEG1 sequence, including exons 1 and 2. The locations of the 5′ and 3′ probes used in Southern analysis screening of transfected ES cell clones are indicated in the top panel. (B) PCR genotyping of mice generated from the mating of heterozygous TIEG1 mutant mice. The arrows indicate the products produced from the wild-type and mutant alleles. (C) Southern blot analysis was performed on genomic DNA from wild-type ($TIEG^{+/+}$), heterozygous ($TIEG^{+/-}$), and homozygous ($TIEG^{-/-}$) TIEG1 mutant mice to verify genotypes. (D) In order to verify loss of TIEG1 expression, Northern analysis was performed as described in Materials and Methods. RNA was extracted from OBs grown in serum-free medium and treated with 2 ng of TGF-β/ml indicated times. (E) Immunoprecipitation analysis was performed from ^{35}S-labeled cell lysates with TIEG-specific polyclonal antibody to demonstrate that $TIEG^{-/-}$ mice did not express TIEG1 protein.

previously (8). Precursors were added to the stromal cells (day 0) by using α-minimal essential medium (Gibco-BRL, Grand Island, N.Y.) supplemented with 10% fetal bovine serum, 1% antibiotic-antimycotic, 10^{-7} M dexamethasone (Sigma Chemical Co., St. Louis, Mo.), and 10^{-5} M vitamin D_3 (BioMol, Plymouth Meeting, Pa.) with or without the addition of 30 ng of RANKL/ml and/or 25 ng of macrophage colony-stimulating factor (M-CSF)/ml as indicated in the figure legends. The medium was changed every 3 days. On day 9, the cocultures were washed three times with 1× PBS (1.7 mM KH_2PO_4, 5 mM Na_2HPO_4, 150 mM NaCl [pH to 7.4]) and fixed with 1% paraformaldehyde in 1× PBS. After incubation for 30 min at room temperature in fixative, the cells were rinsed with water three times and stored in water at 4°C until they were evaluated for differentiation as follows: tartrate-resistant acid phosphatase (TRAP) staining was used to visualize differentiated cells according to the manufacturer's directions (Sigma). The mononuclear and multinucleated TRAP-positive cells were counted by using an Olympus inverted microscope at ×200 magnification.

Real-time PCR analyses. Calvarial cells were plated into six-well plates at a density of 6.4×10^5 cells/well and treated with 10^{-7} M 1,25-dihydroxyvitamin D_3 and 10^{-7} M dexamethasone for 3 days. RNA was isolated by using TRIzol reagent according to the manufacturer's protocol (Invitrogen, Carlsbad, Calif.). After LiCl precipitation to remove DNA, cDNA was synthesized by standard protocol. First, 1 μg of total RNA was heat denatured at 68°C for 15 min in RT reaction buffer [50 mM Tris-HCl, 75 mM KCl, 3 mM $MgCl_2$, 50 mM dithiothreitol, 1 μM deoxynucleoside triphosphates, 500 ng of oligo (dT) primer]. After heat denaturation, 1 U of Moloney murine leukemia virus reverse transcriptase (Invitrogen) was added, and the mixture incubated at 37°C for 45 min, followed by incubation at 68°C for an additional 15 min. Then, 2 μl of the resultant cDNA was used for each reaction as follows: PCR buffer (20 mM Tris-HCl, 50 mM KCl, 3 mM $MgCl_2$), 300 nM concentrations of both the upstream and downstream primers (see below), and 1 U of *Taq* polymerase (Promega). As a control, tubulin was always amplified simultaneously in separate reactions. Message levels were examined by using the Bio-Rad iCycler according to the specifics recommended by the manufacturer. The amount of target cDNA in the sample, relative to tubulin, was calculated by using the formula $2^{\Delta\Delta Ct}$, where ΔΔCt is the fractional cycle number difference between the target and tubulin levels. The results were calculated as the relative quantification of the target gene compared to a control (vehicle without vitamin D or dexamethasone) treatment. The primers used were as follows: M-CSF-F, 5′-CTCTGGCTGGCTTGGCTTGG-3′; M-CSF-R, 5′-GCAGAAGGATGAGGTTGTG-3′; OPG-F, 5′-ACGGACAGCTGGCACACCAG-3′; OPG-R, 5′-CTCACACACTCGGTTGTGGG-3′; RANKL-F, 5′-GGAGGACCATGAACCCTTTCC-3′; RANKL-R, 5′-GCTGGCTGCTGCTTCACTGG-3′; Tubulin-F, 5′-CTGCTCATCAGCAAGATCAGAG-3′; and Tubulin-R, 5′-GCATTATAGGGCTCCACCACAG-3′.

RESULTS

Generation of TIEG1 mutant ES cells and null mice. The 38loxPNeo/TIEG1 construct was transfected into murine ES cells by electroporation. The cells were isolated from the inner cell mass of a 3.5-day 129/SvJ mouse embryo. After expansion in selective growth medium, individual clones were screened by Southern blotting of EcoRI-digested genomic DNA with a probe to a region outside of the targeted locus (5′ probe) to identify clones that contain the correctly targeted TIEG1 allele (Fig. 1A). In addition, a probe to the neomycin resistance gene (Neo^r) was included. One positive clone was identified, expanded, and confirmed by additional Southern analysis with the 3′ probe. As shown in Fig. 1, correct homologous recombination results in a null mutation in which exons 1 and 2, as well as 2.3 kb of 5′-flanking region of mTIEG1 (including transcription and translational start sites and the first 114 amino acids of the TIEG1 protein) was replaced with the Neo^r cassette. In addition, the Neo^r cassette contains a poly(A) termination signal that would terminate transcription of any aberrant mRNA transcript that might be synthesized from the mutant TIEG1 allele. TIEG1 mutant ES cells were used to generate chimeric animals by injection into C57BL/6 (B6) blastocysts as described elsewhere (35).

One male chimera was generated and subsequently bred to B6 females. DNA was isolated from tail biopsies of agouti-colored offspring and screened for germ line transmission of the null allele by PCR and Southern blot. Heterozygous male TIEG1 mutant mice were bred to B6 females to increase the colony size, and subsequent heterozygous male and female mice were interbred to generate homozygotes.

To confirm the TIEG1 gene knockout in mice, genomic DNA was isolated from the tail clippings of $TIEG^{+/+}$, $TIEG^{+/-}$, and $TIEG^{-/-}$ mice. Genotyping of mutant mice was performed by PCR and Southern blot analysis, and the results are shown in Fig. 1B and C. To determine whether TIEG1 mRNA is absent in the TIEG1 null mice, we performed Northern blot analysis on RNA isolated from $TIEG^{+/+}$ and $TIEG^{-/-}$ OBs grown in culture. The osteoblasts were treated with TGF-β1 (2 ng/ml) for various time intervals, as shown on top of each lane in Fig. 1D. As expected, we observed more than 10-fold increase in TIEG1 mRNA levels after 90 min of TGF-β treatment of wild-type osteoblasts, whereas the osteoblasts obtained from TIEG1 null mice displayed no TIEG1 mRNA. A weakly expressed, shorter transcript that hybridized with TIEG1 cDNA in $TIEG^{-/-}$ calvarial OB and other tissues was observed (data not shown). Further analysis of the weakly expressed, shorter transcript demonstrated that TGF-β failed to regulate this transcript in the OB cells. The data suggest that this transcript results from readthrough of the Neo^r cassette and is not regulated by TGF-β. We also performed immunoprecipitation analysis from ^{35}S-labeled OBs treated with TGF-β1 derived from $TIEG^{+/+}$ and $TIEG^{-/-}$ mice. As expected, no TIEG1 protein was expressed in osteoblasts obtained from $TIEG^{-/-}$ mice (Fig. 1E).

Phenotype of TIEG1 null mice. Under gross examination, the TIEG1 null mice are phenotypically normal and the breeding characteristics appear to be normal. Histomorphometric analyses of the tibias (Fig. 2) revealed that the number of osteoblasts, but not of osteoclasts, per cancellous bone surface was significantly higher in the $TIEG^{-/-}$ bones compared to the $TIEG^{+/+}$ bones. However, there was no evidence of elevated bone formation in the $TIEG^{-/-}$ bones on the basis of labeled surface per bone surface, bone formation rate per bone surface or total volume, bone volume per total volume, or mineral apposition rate.

OB cell proliferation. To further characterize the role of TIEG1 in osteoblast gene expression and differentiation, we isolated OBs from $TIEG^{+/+}$ and $TIEG^{-/-}$ mice and cultured in vitro. OBs from $TIEG^{+/+}$ and $TIEG^{-/-}$ mice were plated onto a 96-well cell culture dish, and the proliferation rate was measured at 24, 48, and 72 h. As shown in Fig. 3, the proliferation rates of $TIEG^{-/-}$ OBs were slightly higher than that of $TIEG^{+/+}$ osteoblasts.

Mineralization of OBs in culture. It is well established that treatment of osteoblasts in culture with BMP2 induces mineralized bone nodule formation. To compare bone nodule formation from $TIEG^{+/+}$ and $TIEG^{-/-}$ OBs in culture, the cells were grown in differentiation media for 18 days with BMP2 treatment every third day. The results of the present study are shown in Fig. 4. The $TIEG^{+/+}$ osteoblasts generated distinctive nodule formation in culture, whereas the $TIEG^{-/-}$ osteoblasts lacked the capacity to form mineralized nodules.

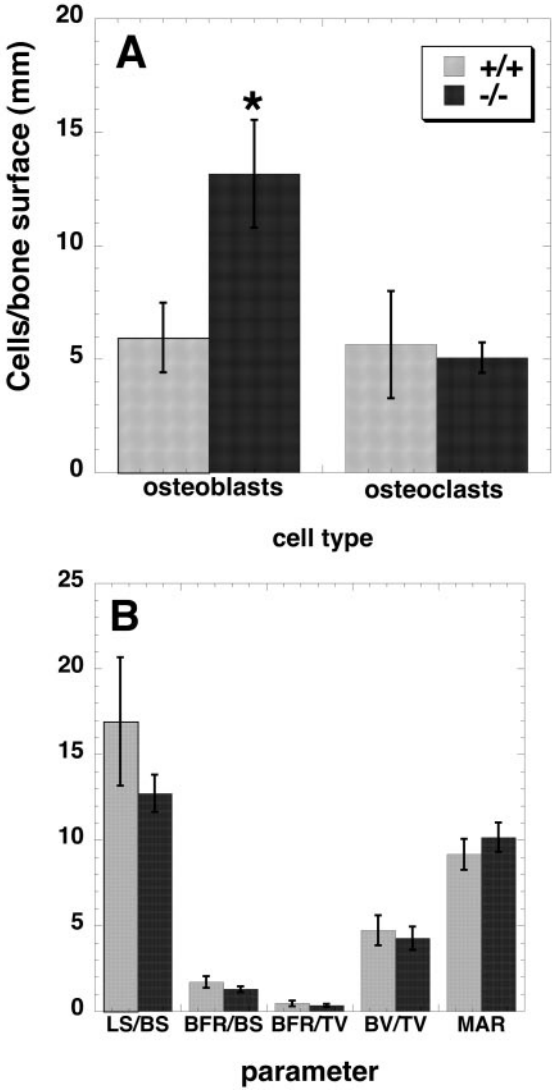

FIG. 2. Histomorphometric analysis of mice. (A) Cell count for osteoblast and osteoclasts per surface area in cancellous bone (in millimeters). (B) Tissue and cellular measurements. The units differ for each data set and were as follows: LS/BS, the percentage of labeled cancellous bone surface per total measured cancellous bone surface; BFR/BS, the amount of new bone formed per week expressed as the percentage of bone surface; BFR/TV, the amount of new bone formed per week expressed as a percentage of total tissue volume; BV/TV, the percentage of cancellous bone volume per measured tissue volume; MAR, mineral apposition rate (>1 μm/week). Data are the means of 5 (+/+) or 6 (−/−) animals ± the SEM. ❋, $P < 0.05$.

TIEG$^{-/-}$ calvarial cells are defective in expression of osteoblastic genes in vitro. The osteoblastic gene expression patterns of the TIEG$^{+/+}$ and TIEG$^{-/-}$ calvarial cells were examined. Total RNA was used to perform log-phase RT-PCR by standard techniques. A representative agarose gel of the bone-related gene products visualized with ethidium bromide is shown in Fig. 5A. Analysis was performed on five separate calvarial isolates, the results were scanned and quantitated by using NIH Image, and the data were normalized to GAPDH (glyceraldehyde-3-phosphate dehydrogenase) expression. Figure 5B represents the calculated mean ± the standard error of the mean (SEM) of the data. Osteocalcin, ostrix, and alkaline phosphatase were significantly lower in the TIEG$^{-/-}$ calvarial cells compared to the TIEG$^{+/+}$ cells. A similar pattern was observed with Cbfa-1, but significant variations in expression between cultures decreased its significance (data not shown). Interestingly, there was no significant difference in type I collagen and GAPDH mRNA levels, demonstrating that TIEG regulates only selected genes. These data explain why the lack of TIEG1 in the OBs reduces the ability of these cells to create bone matrix via a deficiency in the expression of select bone-related (osteoblastic) gene expression.

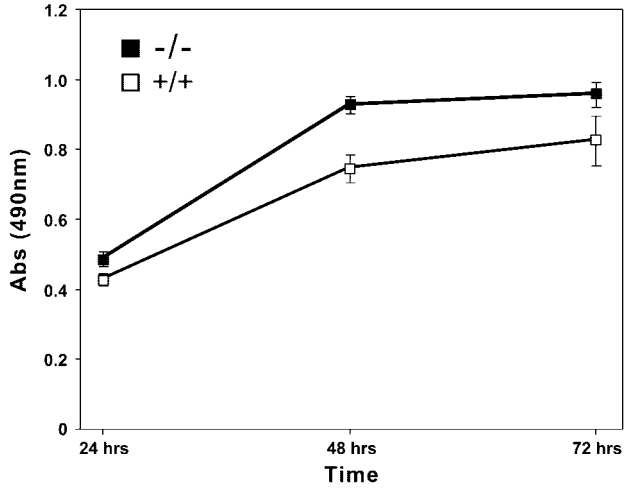

FIG. 3. TIEG$^{+/+}$ and TIEG$^{-/-}$ OBs were plated onto 96-well plates and the cells were grown for 24, 48, and 72 h at 37°C. The proliferation of these cells were measured by using cell titer 96 "the Aqueous One solution for cell proliferation assay" as described in Materials and Methods. An average of six replicates of each were graphed.

Osteoblastic cells from TIEG$^{-/-}$ mice are defective in supporting osteoclast differentiation. Osteoblastic cells from TIEG$^{+/+}$ and TIEG$^{-/-}$ mice were plated, and marrow or spleen tissues from TIEG$^{+/+}$ mice were used as a source of wild-type osteoclast precursors. After coculture in the presence of vitamin D_3 and dexamethasone for 9 days, the number of osteoclasts were determined (Fig. 6). Compared to TIEG$^{+/+}$ osteoblastic cells, TIEG$^{-/-}$ mice cells are significantly less able to support osteoclast differentiation from either marrow or spleen precursors.

The RANKL/OPG ratio is lower in TIEG$^{-/-}$ cells than in TIEG$^{+/+}$ cells. Osteoblastic cells support osteoclast differentiation by producing the enhancers of osteoclast (OC) differentiation, M-CSF and RANKL, with a balanced production of the inhibitor of OC differentiation, osteoprotegerin (OPG), a RANKL decoy receptor (17). Since we utilized vitamin D and dexamethasone to stimulate RANKL and M-CSF expression while repressing OPG expression in support cells, we examined the impact of these hormones on calvarial cell gene expression by using real-time PCR. As shown in Fig. 7, there are reduced RANKL and increased OPG mRNA levels in the TIEG$^{-/-}$ calvarial cells compared to TIEG$^{+/+}$. Thus, a significant reduction in the RANKL to OPG ratio in the TIEG$^{-/-}$ mice compared to TIEG$^{+/+}$ cells. In contrast, there is no apparent impact of lack of TIEG1 on M-CSF gene expression. Exami-

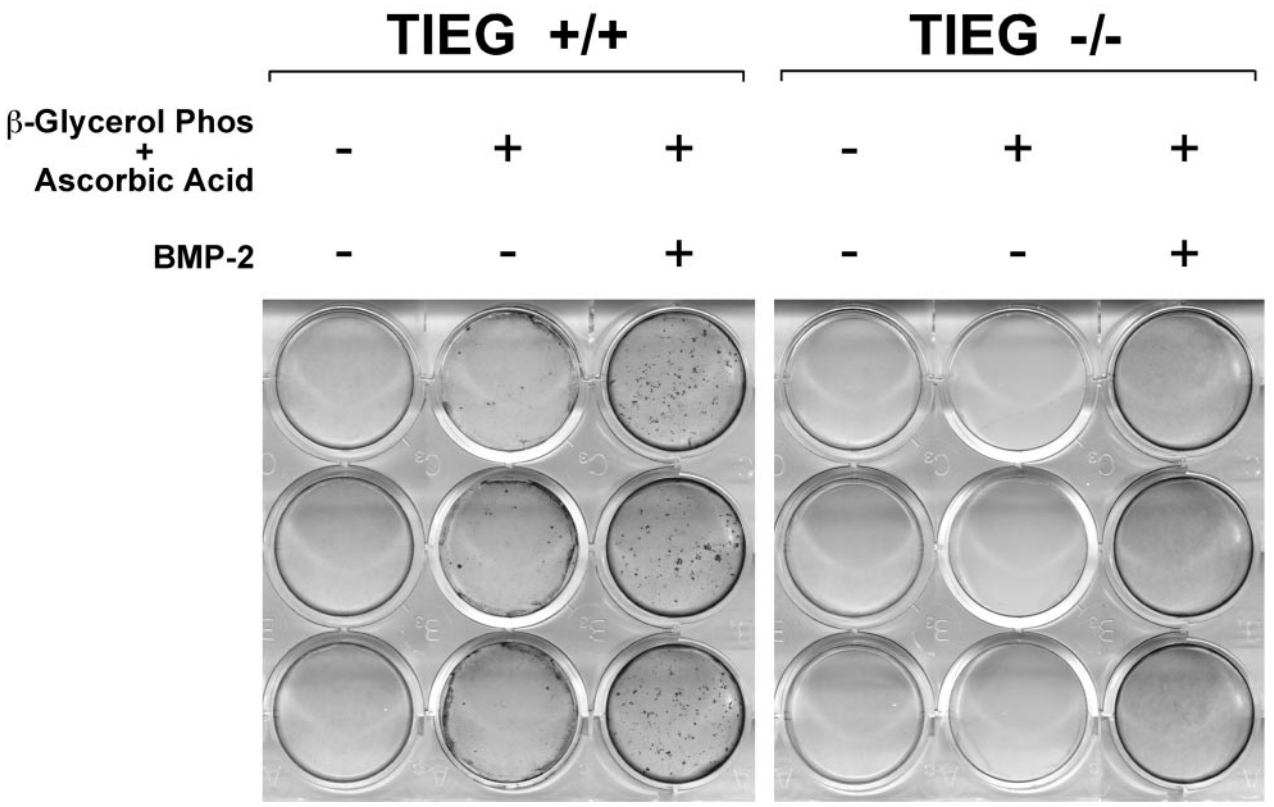

FIG. 4. TIEG$^{+/+}$ and TIEG$^{-/-}$ OBs were grown in differentiation medium with or without BMP2 for 18 days and stained with alizarin red to visualize the bone nodules.

nation of secreted protein levels by using a cytokine array (Ray Biotech, Norcross, Ga.) reveals that there was 2-fold less OPG in TIEG$^{+/+}$ cultures compared to TIEG$^{-/-}$ cultures, whereas there was 3.9-fold more M-CSF in the TIEG$^{+/+}$ cultures compared to TIEG$^{-/-}$ cell cultures (data not shown).

Replenishing the RANKL partially restores the TIEG$^{-/-}$ calvarial cell's ability to induce osteoclast differentiation. The data presented above suggest that either altering the M-CSF (due to protein secretion differences) or the ratio of RANKL to OPG (due to gene and protein differences) could reverse the reduced capacity of the TIEG$^{-/-}$ calvarial cells to support osteoclast differentiation. To examine these possibilities, we cultured TIEG$^{+/+}$ and TIEG$^{-/-}$ OB cells with TIEG$^{+/+}$ marrow in the presence of various combinations of the growth factors (Fig. 8). Addition of 30 ng of RANKL/ml partially, but not completely, restores differentiation. A total of 10 ng of M-CSF/ml given alone or in conjunction with RANKL treatment has no additional impact on osteoclast differentiation versus the effect of the addition of RANKL alone. Additional experiments with higher RANKL concentrations did not increase differentiation above that measured with 30 ng/ml (data not shown).

DISCUSSION

TIEG1 was originally cloned from human osteoblasts as a primary response gene to TGF-β treatment (28). TIEG1 protein overexpression in human osteosarcoma MG63 cells mimicked TGF-β actions on these cells by inducing alkaline phosphatase, decreasing osteocalcin gene expression, and inhibiting cell proliferation, thus supporting a multifaceted role for TIEG1 in osteoblasts (10). In order to understand the physiological role of TIEG1 in development, we generated TIEG1$^{-/-}$ mice through homologous recombination. TIEG1$^{-/-}$ mice are phenotypically normal with regard to breeding characteristics but had skeletal defects such as increased osteoblast numbers per bone surface. The elevated osteoblast numbers in the TIEG$^{-/-}$ bones did not result in an increase in any bone formation parameters measured. These observations are consistent with an impaired ability of the TIEG$^{-/-}$ osteoblasts to form bone. Indeed, isolated OBs exhibited a striking inability to form mineralized modules in vitro after BMP2 treatment. We have documented that BMP2 induces TIEG1 expression in osteoblasts in a manner similar to TGF-β, supporting that the lack of mineralized nodule formation may be directly the result of the loss of TIEG1 in these cells. However, the lower expression levels of alkaline phosphatase, osteocalcin, and two important osteoblast-specific transcription factors Cbfa-1 and osterix are also likely to contribute to the inability of the TIEG$^{-/-}$ osteoblasts to mineralize nodules in vitro. It is also possible that there are other, as-yet-unidentified, alterations that contribute to this phenotype. TIEG1$^{-/-}$ osteoblasts had slightly higher proliferation rates than their wild-type counterpart. Thus, increased proliferation of TIEG$^{-/-}$ osteoblasts in the tibia could be respon-

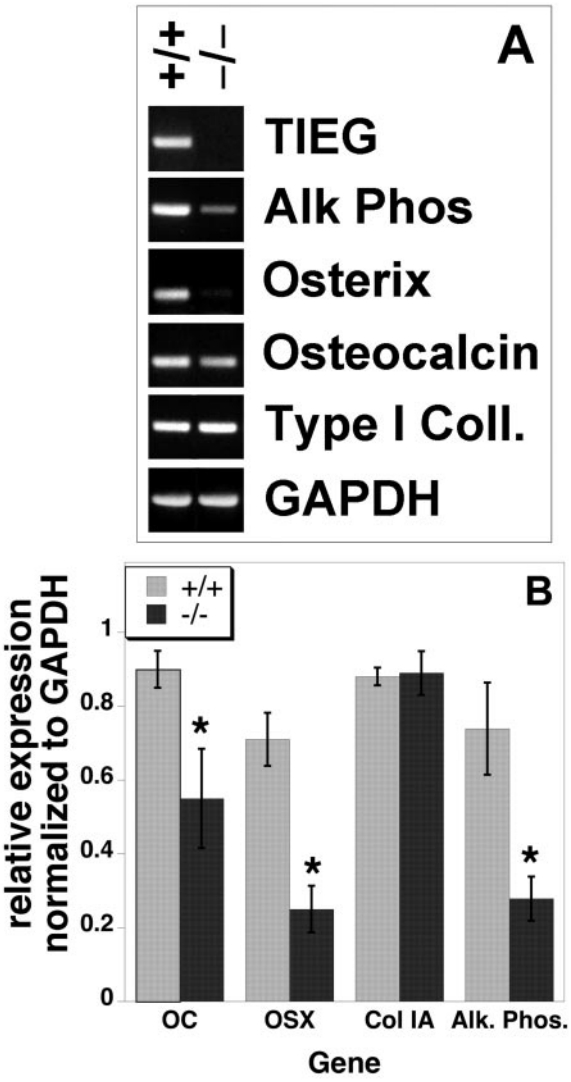

FIG. 5. Total RNA was isolated from TIEG$^{+/+}$ and TIEG$^{-/-}$ OBs grown in culture, and RT-PCR was performed for osteoblast-specific marker genes. (A) Agarose gel of the RT-PCR products as visualized with ethidium bromide. (B) RT-PCR was performed on five separate calvarial RNA isolates, and the results were scanned and quantitated by using NIH Image. The data are the means ± the SEM of these analyses normalized to GAPDH expression. ✻, $P < 0.05$ (comparing TIEG$^{+/+}$ to TIEG$^{-/-}$ OBs).

sible for our observed elevation in osteoblast numbers in the TIEG$^{-/-}$ bones.

Studies in other laboratories with mice lacking other genes have reported similar defects in the osteoblast cells. Zhang et al. (40) characterized the skeleton of Cox-1$^{-/-}$ and Cox-2$^{-/-}$ mice. Cox-1$^{-/-}$ mice exhibited a 60% reduction in intramembranous bone formation when fibroblast growth factor 1 was injected in vivo at the site of the calvaria. Further, these authors showed that bone marrow stromal cells obtained from Cox-2$^{-/-}$ mice exhibited a 50% reduction in bone nodule formation in culture. The reduced nodule formation in Cox-2$^{-/-}$ cells was attributed to the lower expression of Cbfa-1 and osterix gene expression (40). Cbfa-1 is a member of the RUNX

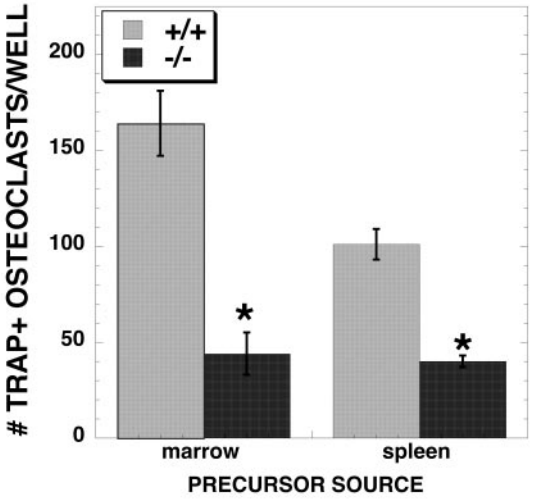

FIG. 6. Knockout OBs are impaired in supporting osteoclast differentiation. Neonatal calvarium-derived osteoblasts from TIEG$^{+/+}$ and TIEG$^{-/-}$ mice were cultured with either marrow or spleen osteoclast precursors from TIEG$^{+/+}$ mice in the presence of vitamin D and dexamethasone for 9 days as described in the text. The data are means ± the SEM of three replicate wells from one experiment. The experiment was performed four times, and these data are representative of the results. ✻, $P < 0.05$ (comparing TIEG$^{+/+}$ to TIEG$^{-/-}$ calvarial cells).

family of transcription factors and plays an important role in osteoblastogenesis, and Cbfa-1$^{-/-}$ mice lack osteoblasts (6, 18). Osterix is another member of the osteoblast-specific transcription factor family and a KLF family member that acts downstream of RUNX2/Cbfa-1 (19). Osterix$^{-/-}$ mice exhibit no bone formation (19). TIEG$^{-/-}$ osteoblasts express less osterix mRNA, although we do not know at this point whether

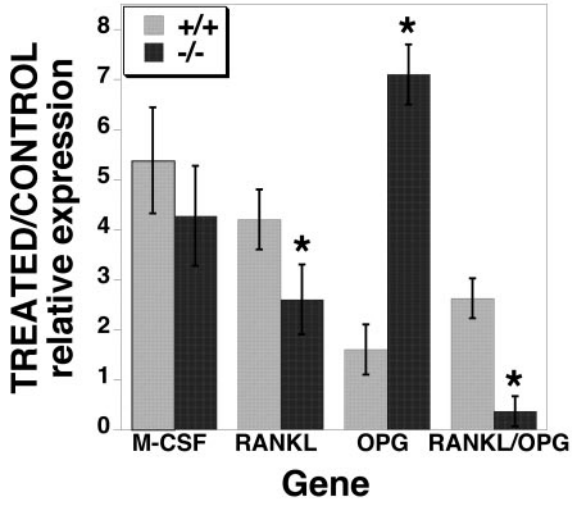

FIG. 7. The RANKL/OPG ratio is lower in TIEG$^{-/-}$ cells than in TIEG$^{+/+}$ cells. Calvarial cells were cultured with (treated) vitamin D and dexamethasone or without treatment (control), followed by RNA isolation as described in the text. Real-time PCR was performed to quantitate the M-CSF, RANKL, and OPG expression relative to tubulin, and the ratio of RANKL to OPG was determined. ✻, $P < 0.05$ (comparing TIEG$^{+/+}$ to TIEG$^{-/-}$ calvarial cells).

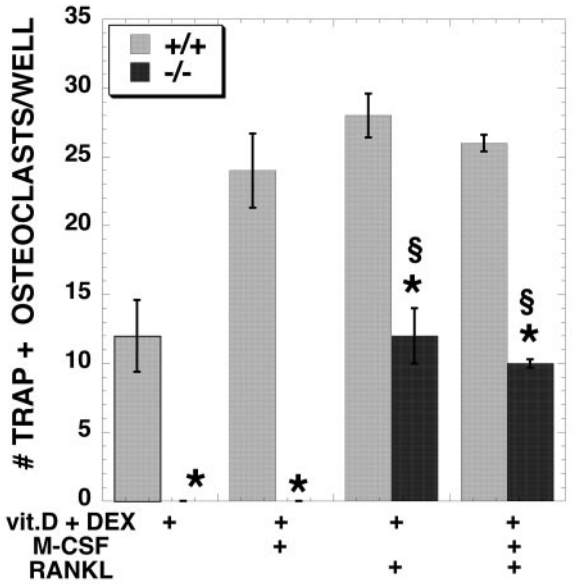

FIG. 8. RANKL partly, but not completely, restores TIEG$^{-/-}$ calvarial cell ability to support osteoclast differentiation. TIEG$^{+/+}$ and TIEG$^{-/-}$ calvarial cells were cultured with TIEG$^{+/+}$ marrow in the presence of the hormones and/or growth factors indicated at the bottom of the figure. *, $P < 0.05$ (comparing TIEG$^{+/+}$ to TIEG$^{-/-}$ calvarial OB cells); §, $P < 0.05$ [comparing vitamin D and dexamethasone alone to addition of the indicated growth factor(s)].

TIEG1 has any direct influence on osterix gene expression. It is possible that TIEG1 is an early primary response gene induced by the members of TGF family, including BMP2, which also regulates osterix at a later period (19). Interestingly, both osterix and TIEG1 belong to the KLF family, and both can bind and compete for the same Sp-1 DNA binding motif sequences to regulate target gene expression (14, 19).

Mice lacking the transcription factor, Sp-3, die immediately after birth due to respiratory failure (9). However, when Sp-3$^{-/-}$ ES cells were allowed to undergo osteogenic differentiation in vitro, bone nodule formation was markedly reduced compared to that of wild-type cells. The authors of that study concluded that this reflects a reduced osteocalcin expression, thereby supporting the idea that Sp-3 is essential for late bone development (9). Wennberg et al. (37) have characterized the primary osteoblasts derived from tissue-nonspecific alkaline phosphatase-deficient (TNAP$^{-/-}$) mice. The osteoblasts derived from these mice exhibited no differences in the protein synthesis or expression of osteoblast-specific marker genes osteopontin, osteocalcin, collagen type I, or Cbfa-1. However, TNAP$^{-/-}$ osteoblasts lacked the ability to mineralize the nodules that they formed in culture. In other studies, Smad3 knockout mice expressed less cortical and cancellous bone compared to wild-type littermates, reflecting osteopenia (2). The decreased rate of bone formation was associated with increased osteocyte number and apoptosis. In the same study, these authors showed that TGF-β was no longer able to inhibit the differentiation of primary osteoblasts derived from Smad3$^{-/-}$ mice.

OBs derived from our TIEG$^{-/-}$ mice lacked the ability to support the osteoclast precursor differentiation to mature osteoclasts. These results imply that TIEG$^{-/-}$ OBs might express the decreased levels of RANKL required for OB support of OC differentiation. To examine this aspect, we isolated RNA from OBs derived from TIEG$^{+/+}$ and TIEG$^{-/-}$ genotypes treated with vitamin D_3 and dexamethasone. When real-time PCR analysis was performed for M-CSF, RANKL, and OPG mRNAs, there were no differences in M-CSF gene expression between TIEG$^{-/-}$ and TIEG$^{+/+}$ osteoblasts, whereas the TIEG$^{-/-}$ cells expressed increased OPG and decreased RANKL mRNA levels. Thus, the RANKL/OPG ratio was greatly reduced in the TIEG$^{-/-}$ osteoblasts. OPG is a secreted glycoprotein that belongs to tumor necrosis factor receptor superfamily and can act as a decoy receptor for RANKL and inhibit osteoclast differentiation and in vivo bone resorption (27). Increased OPG in conjunction with decreased RANKL gene expression might represent a component of the causative factors for the TIEG$^{-/-}$ OBs' inability to support osteoclast differentiation. Interestingly, when the OC differentiation factor, RANKL, was added back into TIEG$^{-/-}$ cocultures, it was able to partially support osteoclasts differentiation. The addition of M-CSF to TIEG$^{-/-}$ cocultures did not have any effect on the restoration of OC differentiation in either the presence or the absence of RANKL. These data support that the lower RANKL to OPG ratio observed in the TIEG$^{-/-}$ mice contributes, in part, to the decreased ability of the TIEG$^{-/-}$ calvarial cells to support osteoclast differentiation. Since RANKL cannot fully restore differentiation to the TIEG$^{+/+}$ level, there must be additional, unidentified, and yet important OB-derived factors lacking in TIEG$^{-/-}$ calvarial cells that contribute to their inability to support differentiation.

It is interesting that we see major differences in OB function, including support for OC differentiation in culture, whereas a minimal skeletal phenotype in vivo was detected. Several humoral factors in vivo are probably compensating for TIEG1. Moreover, TIEG1 might be compensated for by other members of the KLFs, which have also been implicated in skeletal development. This lack of a bone phenotype in mice that have been shown to lack an apparently critical OB factor is not a new observation. Rittling et al. (25) developed osteopontin$^{-/-}$ (OPN$^{-/-}$) mice that did not show an apparent phenotype. When osteoclast precursors, isolated from OPN$^{-/-}$ spleen, were allowed to differentiate in culture to form mature OCs, the OPN$^{-/-}$ mice formed more osteoclasts than OPN$^{+/+}$ mice. In a subsequent study, when these OPN$^{-/-}$ animals were stressed by ovariectomy, OPN$^{-/-}$ mice were resistant to ovariectomy-induced bone resorption compared to wild-type mice (38).

Previously, by using a yeast two-hybrid assay, we demonstrated that TIEG1 binds to SIAH, which is an E_3 ubiquitin ligase and targets TIEG1 for proteosomal degradation (15). House et al. (12) have further shown that SIAH interaction with TIEG1 occurs through a core-binding motif, PxAxVxP, that is present at the N-terminal region of TIEG1 protein. A recent study by Frew et al. (7) showed that SIAH2 knockout mice are phenotypically normal and fertile. Interestingly, SIAH2 mutant bone marrow produces more osteoclasts in vitro than the wild-type. These results are in contrast to those obtained with TIEG$^{-/-}$ mice. It would be interesting to determine whether SIAH2 null mice express increased TIEG1 expression that in turn would support the possibility that TIEG1 might play an important role in osteoclastogenesis.

In summary, we have developed a TIEG$^{-/-}$ mice that display increased osteoblast numbers with no increased bone formation parameters in vivo. Further, we have demonstrated that the osteoblasts and osteoclasts derived from these mice have defects in differentiation. The results of the present study also suggest that TIEG1 expression in osteoblasts is critical for both osteoblast function and OB support of OC differentiation.

ACKNOWLEDGMENTS

Support for this study was provided by NIH grants R01 DE14036 (T.C.S.) and DE14680 (M.J.O.), The Mazza Foundation, and The Mayo Foundation.

We thank Jacquelyn House for excellent clerical assistance and Jean Sibonga for help in histomorphometric analysis.

REFERENCES

1. **Bieker, J. J.** 2001. Krüppel-like factors: three fingers in many pies. J. Biol. Chem. **276:**34355–34358.
2. **Borton, A. J., J. P. Frederick, M. B. Datto, X. F. Wang, and R. S. Weinstein.** 2001. The loss of Smad3 results in a lower rate of bone formation and osteopenia through dysregulation of osteoblast differentiation and apoptosis. J. Bone Miner. Res. **16:**1754–1764.
3. **Chalaeux, E., T. Lopez-Rovira, J. L. Rosa, Pons, G., L. M. Boxer, R. Bartrons, and F. Ventura.** 1999. A zinc-finger transcription factor induced by TGFβ promotes apoptotic cell death in epithelial Mv1Lu cells. FEBS Lett. **457:**478–482.
4. **Cook, T., B. Gebelein, M. Belal, K. Mesa, R., and Urrutia.** 1999. Three conserved transcriptional repressor domains are a defining feature of the TIEG1 subfamily of Sp1-like zinc finger proteins. J. Biol. Chem. **274:**29500–29504.
5. **Dang, D. T., P. Jonathan, and V. W. Yang.** 2000. The biology of the mammalian Krüppel-like family of transcription factors. Int. J. Biochem. Cell Biol. **32:**1103–1121.
6. **Ducy, P., R. Zhang, V. Geoffroy, A. C. Ridall, and G. Karsenty.** 1997. Osf2/Cbfa1: a transcriptional activator of osteoblast differentiation. Cell **89:**747–754.
7. **Frew, I. J., V. E. Hammond, R. A. Dickins, J. M. W. Quinn, C. R. Walkley, N. A. Sims, R. Schnall, N. G. Della, A. J. Holloway, M. R. Digby, P. W. Janes, D. M. Tarlington, L. E. Purton, M. T. Gillespie, and D. D. L. Bowtell.** 2003. Generation and analysis of Siah2 mutant mice. Mol. Cell. Biol. **23:**9150–9161.
8. **Gingery, A., E. Bradley, A. Shaw, and M. J. Oursler.** 2003. Phosphatidylinositol 3-kinase coordinately activates MEK/ERK and AKT/NFKB pathways to maintain osteoclast survival. J. Cell. Biochem. **89:**165–179.
9. **Göllner, H., C. Dani, B. Phillips, S. Philipsen, and G. Suske.** 2001. Impaired ossification in mice lacking the transcription factor SP-3. Mech. Dev. **106:**77–83.
10. **Hefferan, T. E., G. G. Reinholz, D. J. Rickard, S. A. Johnsen, K. M. Waters, M. Subramaniam, and T. C. Spelsberg.** 2000. Over-expression of a nuclear protein, TIEG, mimics transforming growth factor-β action in human osteoblast cells. J. Biol. Chem. **275:**20255–20259.
11. **Hoovers, J. M., M. Mannens, R. John, J. Bliek, V. van Heyningen, D. J. Porteous, N. J. Leschot, A. Westerveld, and P. F. Little.** 1992. High resolution localization of 69 potential human zinc finger protein genes: a number are clustered. Genomics **12:**254–263.
12. **House, C. M., I. J. Frew, H.-L. Huang, G. Wiche, N. Traficante, E. Nice, B. Catimel, and D. D. L. Bowtell.** 2003. A binding motif for Siah ubiquitin ligase. Proc. Natl. Acad. Sci. USA **100:**3101–3106.
13. **Jin, W., L. Qu, P. Min, S. Chen, H. Li, H. Lu, and Y. Hou.** 2004. Identification of genes responsive to apoptosis in HL-60 cells. Acta Pharmacol. Sin. **25:**319–326.
14. **Johnsen, S. A., M. Subramaniam, R. Janknecht, and T. C. Spelsberg.** 2002. TGFβ inducible early gene enhances TGFβ/Smad dependent transcriptional responses. Oncogene **21:**5783–5790.
15. **Johnsen, S. A., M. Subramaniam, D. G. Monroe, R. Janknecht, and T. C. Spelsberg.** 2002. Modulation of TGFβ/Smad transcriptional responses through targeted degradation of the TGFβ inducible early gene-1 by the human *seven in absentia* homologue. J. Biol. Chem. **277:**30754–30759.
16. **Johnsen, S. A., M. Subramaniam, T. Katagiri, R. Janknecht, and T. C. Spelsberg.** 2002. Transcriptional regulation of Smad2 is required for enhancement of TGFβ/Smad signaling by TGFβ inducible early gene. J. Cell. Biochem. **87:**233–241.
17. **Khosla, S.** 2001. Minireview: the OPG/RANKL/RANK system. Endocrinology **142:**5050–5055.
18. **Komori, T. H. Yagi, S. Nomura, A. Yamaguchi, K. Sasaki, K. Deguchi, Y. Shimizu, R. T. Bronson, Y. H. Gao, M. Inada, M. Sato, R. Okamoto, Y. Kitamura, S. Yoshiki, and T. Kishimoto.** 1997. Targeted disruption of Cbfa1 results in a complete lack of bone formation owing to maturational arrest of osteoblasts. Cell **89:**755–764.
19. **Nakashima, K. X. Zhou, G. Kunkel, Z. Zhang, J. M. Deng, R. R. Behringer, and D. de Crombrugghe.** 2002. The novel zinc finger-containing transcription factor osterix is required for osteoblast differentiation and bone formation. Cell **108:**17–29.
20. **Noti, J. D., A. K. Johnson, and J. D. Dillon.** 2004. The zinc-finger transcription factor TIEG1 confers myeloid-specific activation of the leukocyte integrin CD11d promoter. J. Biol. Chem. **279:**26948–26958.
21. **Parfitt, A., M. Drezner, F. Glorieux, J. Kanis, H. Malluche, P. Meunier, S. Ott, and R. Recker.** 1987. Bone histomorphometry: standardization of nomenclature, symbols, and units. J. Bone Miner. Res. **2:**595–610.
22. **Reinholz, M. M. M. W. An, S. A. Johnsen, M. Subramaniam, V. J. Suman, J. N. Ingle, P. C. Roche, and T. C. Spelsberg.** 2004. Differential gene expression of TGFβ inducible early gene (TIEG), Smad 7, Smad 2, and Bard 1 in normal and malignant breast tissue. Breast Cancer Res. Treatment **166:**1–14.
23. **Ribeiro, A., S. F. Bronk, P. J. Roberts, R. Urrutia, and G. J. Gores.** 1999. The transforming growth factor β1-inducible transcription factor, TIEG1, mediates apoptosis through oxidative stress. Hepatology **30:**1490–1497.
24. **Rickard, D. J., D. G. Monroe, T. J. Ruesink, S. Khosla, B. L. Riggs, and T. C. Spelsberg.** 2003. Phytoestrogen genistein acts as an estrogen agonist on human osteoblastic cells through estrogen receptors α and β. J. Cell. Biochem. **89:**633–646.
25. **Rittling, S. R., H. N. Matsumoto, M. D. McKee, A. Nanci, X. R. An, K. E. Novick, A. J. Kowalski, M. Noda, and D. T. Denhardt.** 1998. Mice lacking osteopontin show normal development and bone structure but display altered osteoclast formation in vitro. J. Bone Miner. Res. **13:**1101–1111.
26. **Sambrook, J., E. F. Fritsch, and T. Maniatis.** 1982. Molecular cloning: a laboratory manual, p. 382–389. Cold Spring Harbor Laboratory Press, Cold Spring Harbor, N.Y.
27. **Simonet, W. S., D. L. Lacey, C. R. Dunstan, M. Kelley, M. S. Chang, R. Luthy, H. Q. Nguyen, S. Wooden, L. Bennett, T. Boone, G. Shimamoto, M. DeRose, R. Elliott, A. Colombero, H. L. Tan, G. Trail, J. Sullivan, E. Davey, N. Bucay, L. Renshaw-Gregg, T. M. Hughes, D. Hill, W. Pattison, P. Campbell, and W. J. Boyle.** 1997. Osteoprotegerin: a novel secreted protein involved in the regulation of bone density. Cell **89:**309–319.
28. **Subramaniam, M., S. A. Harris, M. J. Oursler, K. Rasmussen, B. L. Riggs, and T. C. Spelsberg.** 1995. Identification of a novel TGFβ regulated gene encoding a putative zinc finger protein in human osteoblasts. Nucleic Acids Res. **23:**4907–4912.
29. **Subramaniam, M., T. E. Hefferan, K. R. Tau, D. Peus, M. Pittelkow, S. Jalal, B. L. Riggs, P. Roche, and T. C. Spelsberg.** 1998. Tissue, cell type, and breast cancer stage-specific expression of a TGFβ inducible early transcription factor gene. J. Cell. Biochem. **68:**226–236.
30. **Tachibana, I., M. Imoto, P. N. Adjei, G. J. Gores, M. Subramaniam, T. C. Spelsberg, and R. Urrutia.** 1997. Over-expression of the TGFβ-regulated zinc finger encoding gene, TIEG, induces apoptosis in pancreatic epithelial cells. J. Clin. Investig. **99:**2365–2374.
31. **Tau, K. R., T. E. Hefferan, K. M. Waters, J. A. Robinson, M. Subramaniam, B. L. Riggs, and T. C. Spelsberg.** 1998. Estrogen regulation of a TGFβ inducible early gene that inhibits DNA synthesis in human osteoblasts. Endocrinology **139:**1346–1353.
32. **Turner, J., and M. Crosley.** 1999. 1999. Mammalian Krüppel-like transcription factors: more than just a pretty finger. Trends Biochem. Sci. **24:**236–240.
33. **Turner, R. T., G. L. Evans, J. P. Sluka, M. D. Adrian, H. U. Bryant, C. H. Turner, and M. Sato.** 1998. Differential responses of estrogen target tissues in rats including bone to clomiphene, enclomiphene, and zuclomiphene. Endocrinology **139:**3712–3720.
34. **Turner, R. T., and G. L. Evans.** 2000. 2-Methoxyestradiol inhibits longitudinal bone growth in normal female rats. Calcif. Tissue Intl. **66:**465–469.
35. **van Deursen, J., A. Heerschap, F. Oerlemans, W. Ruitenbeck, P. Jap, H. ter Laak, and B. Wieringa.** 1993. Skeletal muscles of mice deficient in muscle creatine kinase lack burst activity. Cell **74:**621–631.
36. **Wang, Z., B. Peters, S. Klussmann, H. Bender, A. Gerb, and K. Krieglstein.** 2004. Gene structure evolution of TIEG3, a new member of the TIEG1 family. Gene **325:**25–34.
37. **Wennberg, C., L. Hessle, P. Lundberg, S. Mauro, S. Narisawa, U. H. Lerner, and J. L. Millan.** 2000. Functional characterization of osteoblasts and osteoclasts from alkaline phosphatase knockout mice. J. Bone Miner. Res. **15:**1879–1888.
38. **Yoshitake, H., S. R. Rittling, D. T. Denhardt, and M. Noda.** 1999. Osteopontin-deficient mice are resistant to ovariectomy-induced bone resorption. Proc. Natl. Acad. Sci. USA **96:**8156–8160.
39. **Zhang, J.-S., M. C. Moncrieffe, J. Kaczynski, V. Ellenrieder, F. G. Prendergast, and R. Urrutia, R.** 2001. A conserved α-helical motif mediates the interaction of Sp1-like transcriptional repressors with the corepressor mSin3A. Mol. Cell. Biol. **21:**5041–5049.
40. **Zhang, X., E. M.Schwarz, D. A. Young, J. E. Puzas, R. N. Rosier, and R. J. O'Keefe.** 2002. Cyclooxygenase-2 regulates mesenchymal cell differentiation into the osteoblast lineage and is critically involved in bone repair. J. Clin. Investig. **109:**1405–1415.